Letter to the Editor

A case study of unexplained multiple hepatoid adenocarcinoma of the bone

Qiao Xie[1#], Limei Wang[1#], Jie Cheng[1], Wei Chen[1], Ping Cai[1], Huarong Zhang[2], Xiaoming Li[1]

[1]7T Magnetic Resonance Translational Medicine Research Center, Department of Radiology, Southwest Hospital, Army Medical University (Third Military Medical University), Chongqing, China; [2]Institute of Pathology and Southwest Cancer Center, Southwest Hospital, Third Military Medical University (Army Medical University), Chongqing, China

[#]These authors contributed equally to this work.

Correspondence to: Ping Cai, PhD; Xiaoming Li, MD. 7T Magnetic Resonance Translational Medicine Research Center, Department of Radiology, Southwest Hospital, Army Medical University (Third Military Medical University), Gaotanyan Street, Shapingba District, Chongqing 400038, China. Email: 530305942@qq.com; 359261069@qq.com; Huarong Zhang, PhD. Institute of Pathology and Southwest Cancer Center, Southwest Hospital, Third Military Medical University (Army Medical University), Gaotanyan Street, Shapingba District, Chongqing 400038, China. Email: 13677653886@163.com.

Submitted Feb 19, 2024. Accepted for publication Jul 25, 2024. Published online Aug 28, 2024.
doi: 10.21037/qims-24-321
View this article at: https://dx.doi.org/10.21037/qims-24-321

Introduction

Hepatoid adenocarcinoma (HAC) is a rare type of malignant adenocarcinoma that originates in extrahepatic tissues or organs, exhibiting histopathological similarities to hepatocellular carcinoma (HCC). Alpha-fetoprotein (AFP)-producing gastric adenocarcinoma was first reported by Bourreille *et al.* (1) in 1970. Subsequently, in 1990, Ishikura *et al.* (2) introduced the concept of hepatoid adenocarcinoma of the lung (HAL). HAC is characterized by a propensity for liver and lymph node metastasis, resulting in poor prognosis. It predominantly affects middle-aged and elderly males, with a median age of onset at 56 years. HAC can develop in various organs, including the stomach (63%), ovary (10%), lung (5%), gallbladder (4%), pancreas (4%), and uterus (4%) (3). Previous studies have identified that HAC could metastasize to the bone, and imaging examinations often reveal the primary lesion (4,5); however, multifocal bone HAC of unknown origin was not reported. Herein, we describe a case of a patient presenting with unexplained multiple bone HAC.

Case presentation

All procedures performed in this study were in accordance with the ethical standards of the institutional and/or national research committee(s) and with the Helsinki Declaration (as revised in 2013). Written informed consent was provided by the patient for publication of this article and accompanying images. A copy of the written consent is available for review by the editorial office of this journal.

A 58-year-old female patient presented with an unexplained onset of poor appetite, accompanied by vomiting and fatigue after eating in November 2020, with no abdominal pain, hematemesis, or melena, and she denied any history of fever or chest pain. The patient had no history of alcohol consumption and hepatitis. The laboratory investigation revealed that thyroid function was normal. Blood routine: basophils count 0.13×10^9/L [normal range, $(0–0.06)\times10^9$/L], red blood cell (RBC) count 2.07×10^{12}/L [normal range, $(3.8–5.1)\times10^{12}$/L], hemoglobin 64 g/L (normal range, 115–150 g/L), platelet count 13×10^9/L [normal range, $(125–350)\times10^9$/L]; hepatitis B core antibody (HBcAb) (+), hepatitis B surface antibody (HBsAb) (+), hepatitis B surface antigen (HBsAg) (–), hepatitis B e-antibody (HBeAb) (–), and hepatitis B e-antigen (HBeAg) (–). Testing for tumor markers revealed the following: CYFRA21-1 23.31 μg/L (normal range, 0–5 μg/L), AFP 39.58 μg/L (normal range, 0–20 μg/L).

Glucose-Glucose: 6.60 mmol/L (normal range, 3.9–6.1 mmol/L). Further blood testing revealed the following: indirect bilirubin 18.80 μmol/L (normal range, 3–16 umol/L), total bilirubin 22.70 μmol/L (normal range, 6–21 μmol/L), alkaline phosphatase (ALP) 2,328 IU/L (normal range, 50–135 IU/L), lactate dehydrogenase (LDH) 671.80 IU/L (normal range, 114–240 IU/L). Abdominal ultrasonography showed no lesions in the liver or cirrhotic changes. Chronic inflammation of the upper part of the gastric body was shown by electron gastroscopy; the mucosa of the duodenal bulb and the descending portion were smooth, with no evidence of erosion or ulceration. Owing to the continuous low counts of RBC, white blood cells (WBC), and platelets, as evidenced by the blood routine examination, and particularly the severely diminished platelet count, the patient was unable to undergo an electronic colonoscopy.

Enhanced computed tomography (CT) examination (Optima CT660 scanner; GE HealthCare, Chicago, IL, USA) was performed with the following parameters: tube voltage 120 kVp, tube current 125–300 mAs, scanning layer thickness 5 mm, reconstruction interval 1.25 mm), and showed that diffuse osteolytic and osteogenic bone destructions involving ribs, sternum, scapulae, vertebrae, pelvic, and femoral bones (*Figure 1A-1C*), with persistent enhancement. No obvious lesions were observed in the liver or gastrointestinal tract on enhanced CT. Additionally, no lesions were detected in the lungs, gallbladder, pancreas, spleen, kidneys, uterine appendages, and bladder.

The positron emission tomography/computed tomography (PET/CT) imaging (*Figure 1D*) revealed multiple osteolytic lesions involving the vertebrae, sternum, bilateral humeri, scapulae, multiple ribs, pelvis, and bilateral femora, with increased fluorodeoxyglucose (FDG) uptake, exhibiting a maximum standard uptake value (SUV) value of 3.47. No abnormal FDG uptake was observed in the liver and gastrointestinal tract.

The patient underwent a CT-guided sacral puncture. The histopathology indicated poorly differentiated carcinoma with nested, pleomorphic polygonal cells with eosinophilic or clear cytoplasm and hyperchromatic nuclei (*Figure 1E,1F*). Immunohistochemical staining showed that the tumor cells were strongly positive for pan cytokeratin (CK) (*Figure 1G*), CK19 (*Figure 1H*), HepPar1 (*Figure 1I*), CK20, CK8/18, CDX2, and scattered positive expression of AFP (*Figure 1J*), and negative for Glypican-3, CD10, CK5/6, CK7, Her-2, CD68, PAX-8, GATA3, TTF-1, P63, SALL4, LIN28, vimentin, and SATB2. Finally, multiple bone HACs were considered as a clinical diagnosis.

The patient underwent treatment with sintilimab plus apatinib and received radiotherapy to the sacrum and ilium. Radiotherapy was suspended due to myelosuppression and a reduction in platelets (Grade IV). Due to the patient's tendency to bleed from the eyelids, the treatment regimen was changed to gefitinib plus sintilimab for 3 cycles. Simultaneously, the patient received treatment to inhibit gastric acid, control nausea and vomiting, protect the gastric mucosa, and provide nutritional support and adjunctive anti-tumor therapy. After the treatment, a contrast-enhanced CT scan of the chest and abdomen (*Figure 2A-2C*) showed that the previously observed areas of osteolytic destruction had diminished in extent and increased in density. However, the patient died of shock in July 2021.

Discussion

This is the first reported case of unexplained multiple bone HAC, the pathogenesis of which remained unclear. Previous literature (4,5) reported that bone metastasis could occur in HAL and HAC of the ovary; however, enhanced CT and PET/CT examinations did not reveal any primary tumor in the lungs or ovaries. A report indicated that the stomach was most common site for HAC (3); however, enhanced CT, PET/CT, and gastroscopy did not reveal any tumor originating from stomach. Additionally, Li *et al.* (3) reported that both the liver and gastrointestinal tract derive from the primitive foregut, so intestinal tract cancer might undergo de-differentiation to hepatocytes in the early embryonic stage, resulting in the formation of HAC. Meanwhile, Sinard *et al.* (6) observed that HAC could occur in tissues and organs not derived from the foregut, and Alison *et al.* (7) suggested that hepatocytes could be derived from bone marrow stem cells. Therefore, we speculated that the multifocal HAC might also originate from bone. AFP could be elevated in HAC; Yang *et al.* indicated that high serum AFP level was an independent risk factor for the prognosis of HAC, and the optimal threshold value of AFP for 3-year overall survival and recurrence-free survival was 516 ng/mL (8). In our current case, the patient had mildly elevated serum AFP (39.14 ng/mL), but did not have any history of chronic liver disease; none of the imaging examinations revealed any liver lesions or cirrhosis, which led us to believe that elevated AFP might be associated with HAC. However, the overall survival of the patient was short (only 8 months), which suggested that a large-sample size study would be needed to determine whether the prognosis

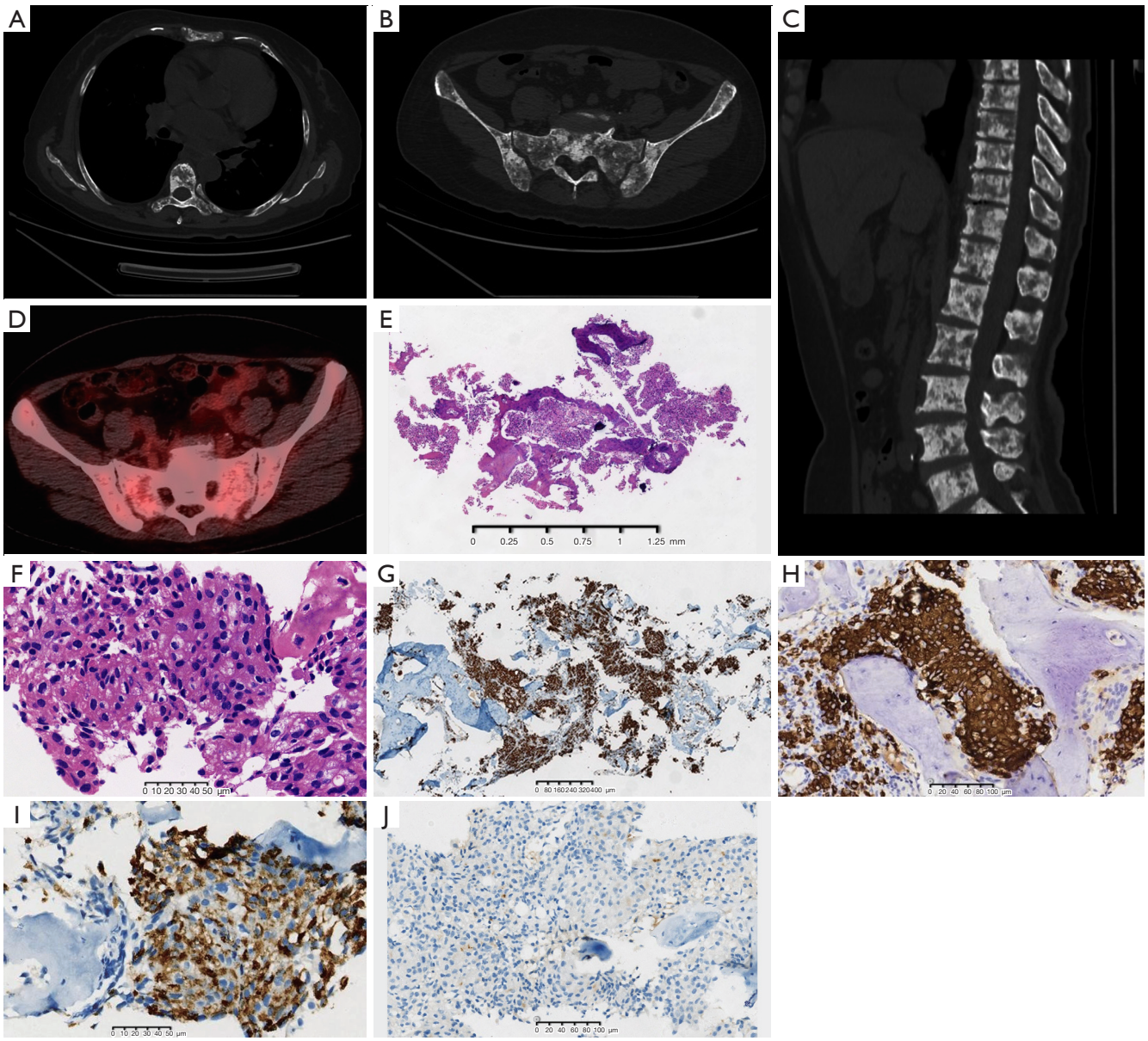

Figure 1 Abdominal enhanced CT, PET/CT, and pathology images of a 58-year-old female patient with multiple bone HAC of unknown etiology. The enhanced CT scan (A-C) revealed multiple osteolytic and osteoblastic bone destructions involving the thoracolumbar spine, sacrum, ribs, scapula, sternum, and hip bones, with unclear boundaries. The PET/CT scan (D) showed increased FDG uptake in the sacrum and bilateral iliac bones within the areas of bone destruction. Histopathology (E,F) showed that the tumor cells were poorly differentiated cancer cells with nested, pleomorphic polygonal cells, eosinophilic or hyaline cytoplasm, and pigmented nuclei (HE ×40, ×400). Immunohistochemistry (G-J) showed pan CK (+) (×50), CK19 (+) (×200), and HepPar1 (+) (×400), and scattered positive expression of AFP (×200). CT, computed tomography; PET/CT, positron emission tomography/computed tomography; HAC, hepatoid adenocarcinoma; FDG, fluorodeoxyglucose; HE, hematoxylin and eosin staining; CK, cytokeratin; AFP, alpha-fetoprotein.

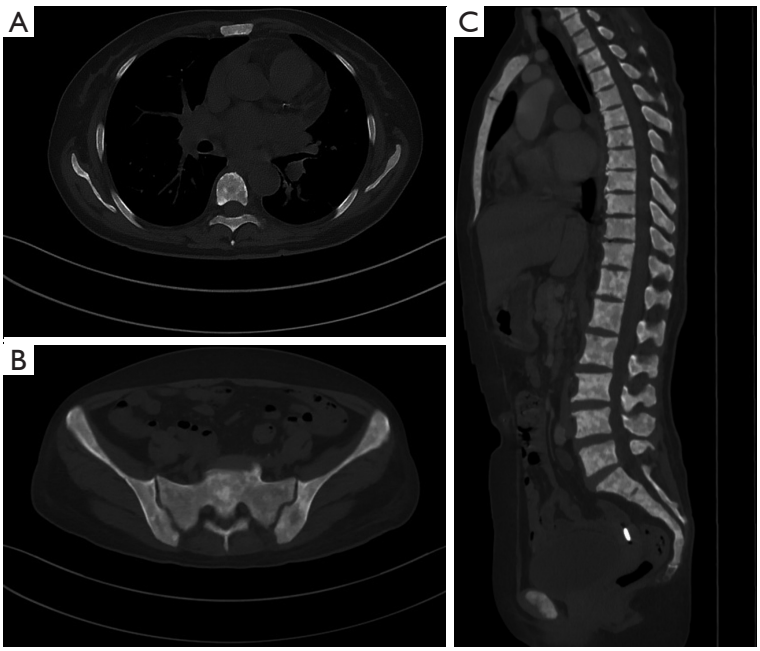

Figure 2 Chest and enhanced CT images after treatment. The CT scans (A-C) demonstrated a significant reduction in the extent of osteolytic bone destruction in the thoracolumbar spine, sacrum, ribs, scapulae, sternum, and hip bones, accompanied by increased density. CT, computed tomography.

of HAC was related to the site of the tumor.

Pathological examination has represented the gold standard for the definitive diagnosis of HAC (3). The typical histomorphology of HAC is characterized by HCC-like differentiation and adenocarcinoma-like differentiation, which are spatially adjacent and migratory to each other. HCC-like differentiation is characterized by large, polygonal tumor cells with eosinophilic or clear cytoplasm, large, darkly stained nuclei, arranged in nested clusters or trabecular patterns, with stroma rich in capillaries and sinusoids, the cancer cells might show steatosis or produce "bile-like" secretions, and the areas of adenocarcinoma-like differentiation manifest as tubular and/or papillary adenocarcinomas, predominantly of low differentiation (3,9), consistent with the pathological morphology of the case in this study. Furthermore, immunohistochemistry (IHC) aided the diagnosis of HAC. Su *et al.* (9) reported that HAC expressed several different markers, including Glypican-3 (100%), AFP (91.6%), HepPar1 (38.1%), CEA (78.7%), CK7 (15.4%), CK18 (100%), CK19 (100%), CK20 (28.6%), α1-AT (91%), and CD10 (62.5%). In this patient, IHC showed positive expression for pan CK, HepPar1, CK19, CK20, CK8/18, and CDX-2 and scattered positive expression of AFP. This was a difficult case, and our diagnostic route was as follows: First, the patient had no history of chronic liver disease, and ultrasonography, enhanced CT, and PET/CT did not reveal any liver lesions or cirrhosis; combined with the pathology, we ruled out bone metastases from the liver. Second, the patient's serum AFP was elevated, and based on the pathological histology and IHC results, common types of cancer of the digestive, respiratory, female reproductive systems, and breast were excluded. Although SALL4 has been shown to be highly sensitive and specific for the diagnosis of HAC of the stomach (HAS) (3), it has shown negative or scattered expression for HAC in the esophagus, intestine, pancreas, biliary tree, mediastinum, and ovary (10-12), so we hypothesized that the negative expression of SALL4 in this case might be related to its cryptogenic primary tumor site or inadequate puncture sampling. Although the positive expression of HepPar1, CK19, and CDX-2 suggested that the tumor might be gastrointestinal differentiation (9,13), the pathological results revealed an absence of adenotubular structures, and negative expression of CK7, STAB2, and HER-2, so we considered a diagnosis of HAS to be less likely. Therefore, it was very difficult to decide whether the multiple HACs originated from bones or other occult metastases.

These multifocal HACs affected nearly the entire skeletal system. The CT scan revealed the coexistence of osteolytic and osteoblastic bone destruction with unclear boundaries, whereas the osteoblastic regions exhibited cotton ball-like high-density shadows. The lesions demonstrated persistent enhancement on enhanced CT, which could easily have been confused with myeloma, a metabolic bone disease. However, the imaging of multiple myeloma typically shows bone destruction without osteoblastic changes (14). Metabolic bone diseases might present as secondary osteoporosis, osteomalacia, bone destruction, or osteosclerosis, with bone destruction and bone proliferation not occurring simultaneously (15).

The high-grade nature of HAC is characterized by its aggressive behavior and poor prognosis, with no standardized treatment guidelines (3). Typically, solitary HAC is managed through surgical resection. For patients in the advanced stages or those ineligible for surgical intervention, chemotherapy and radiotherapy are employed to prolong survival. In this case, as the extensive lesions were not amenable to surgical treatment, a combination of chemotherapy and radiotherapy was administered, and follow-up CT revealed the presence of bone repair; however, the patient died of shock within a short period of time.

Conclusions

Multiple bone HAC is extremely rare. When a patient presents with concurrent osteoblastic and osteolytic bone destruction accompanied by elevated AFP levels, even if the primary lesion is unclear, clinicians should suspect bone HAC and proceed with imaging, pathological, and genetic examinations for individualized treatment.

Acknowledgments

Funding: This study received funding from the Program of the National Natural Science Foundation of Chongqing (No. CSTB2022NSCQMSX1371).

Footnote

Conflicts of Interest: All authors have completed the ICMJE uniform disclosure form (available at https://qims.amegroups.com/article/view/10.21037/qims-24-321/coif). All authors report that this study was supported by the Program of the National Natural Science Foundation of Chongqing (No. CSTB2022NSCQMSX1371). The authors have no other conflicts of interest to declare.

Ethical Statement: The authors are accountable for all aspects of the work in ensuring that questions related to the accuracy or integrity of any part of the work are appropriately investigated and resolved. All procedures performed in this study were in accordance with the ethical standards of the institutional and/or national research committee(s) and with the Helsinki Declaration (as revised in 2013). Written informed consent was provided by the patient for publication of this article and accompanying images. A copy of the written consent is available for review by the editorial office of this journal.

References

1. Bourreille J, Metayer P, Sauger F, Matray F, Fondimare A. Existence of alpha feto protein during gastric-origin secondary cancer of the liver. Presse Med (1893) 1970;78:1277-8.
2. Ishikura H, Kanda M, Ito M, Nosaka K, Mizuno K. Hepatoid adenocarcinoma: a distinctive histological subtype of alpha-fetoprotein-producing lung carcinoma. Virchows Arch A Pathol Anat Histopathol 1990;417:73-80.
3. Li M, Mei YX, Wen JH, Jiao YR, Pan QR, Kong XX, Li J. Hepatoid adenocarcinoma-Clinicopathological features and molecular characteristics. Cancer Lett 2023;559:216104.
4. Lazaro J, Rubio D, Repolles M, Capote L. Hepatoid carcinoma of the ovary and management. Acta Obstet Gynecol Scand 2007;86:498-9.
5. Haninger DM, Kloecker GH, Bousamra Ii M, Nowacki MR, Slone SP. Hepatoid adenocarcinoma of the lung: report of five cases and review of the literature. Mod Pathol 2014;27:535-42.
6. Sinard J, Macleay L Jr, Melamed J. Hepatoid adenocarcinoma in the urinary bladder. Unusual

localization of a newly recognized tumor type. Cancer 1994;73:1919-25.
7. Alison MR, Poulsom R, Jeffery R, Dhillon AP, Quaglia A, Jacob J, Novelli M, Prentice G, Williamson J, Wright NA. Hepatocytes from non-hepatic adult stem cells. Nature 2000;406:257.
8. Yang X, Wang A, Li J, Zhou K, Ji K, Ji X, Zhang J, Wu X, Bu Z. Prognostic significance of preoperative serum tumor markers in hepatoid adenocarcinoma of stomach (HAS). BMC Cancer 2023;23:53.
9. Su JS, Chen YT, Wang RC, Wu CY, Lee SW, Lee TY. Clinicopathological characteristics in the differential diagnosis of hepatoid adenocarcinoma: a literature review. World J Gastroenterol 2013;19:321-7.
10. Mattiolo P, Scarpa A, Luchini C. Hepatoid tumors of the gastrointestinal/pancreatobiliary district: morphology, immunohistochemistry, and molecular profiles. Hum Pathol 2023;132:169-75.
11. Zhang G, Wen C, Chen B, Dai H, Lin R, Huang Y, Xiang X. Mediastinal Hepatoid Adenocarcinoma Treated With Arterial Interventional Therapy: A Case Report and Review of Literature. Front Oncol 2022;12:785888.
12. Acosta AM, Pins MR. Hepatoid Carcinoma of the Ovary: Clinical, Histopathologic, and Immunophenotypic Features. Arch Pathol Lab Med 2019;143:883-9.
13. Kmeid M, Lukose G, Hodge K, Cho D, Kim KA, Lee H. Aberrant expression of SATB2, CDX2, CDH17 and CK20 in hepatocellular carcinoma: a pathological, clinical and outcome study. Histopathology 2021;79:768-78.
14. Maggialetti N, Ferrari C, Nappi AG, Quinto A, Rossini B, Zappia M, Minoia C, Guarini A, Brunese L, Rubini G. Is whole body low dose CT still necessary in the era of (18)F-FDG PET/CT for the assessment of bone disease in multiple myeloma patients? Hell J Nucl Med 2020;23:264-71.
15. Jevtic V. Imaging of renal osteodystrophy. Eur J Radiol 2003;46:85-95.

Cite this article as: Xie Q, Wang L, Cheng J, Chen W, Cai P, Zhang H, Li X. A case study of unexplained multiple hepatoid adenocarcinoma of the bone. Quant Imaging Med Surg 2024;14(9):7018-7023. doi: 10.21037/qims-24-321

